Possible $\Sigma^*(\frac{1}{2}^-)$ in the initial-state polarized $\gamma N \to K^+\Sigma^*(1385) \to K^+\pi\Lambda$ reaction near threshold

Yun-Hua Chen[1] and B. S. Zou[1,2]

[1]*Institute of High Energy Physics, CAS, P.O. Box 918(4), Beijing 100049, China*

[2]*State Key Laboratory of Theoretical Physics, Institute of Theoretical Physics, CAS, Beijing 100190, China*

(Received 21 February 2013; revised manuscript received 22 June 2013; published 5 August 2013)

By using an effective Lagrangian method, we study the effects of a newly proposed $\Sigma^*(\frac{1}{2}^-)$ state with mass around 1380 MeV in the initial-state polarized $\gamma N \to K^+\Sigma^*(1385) \to K^+\pi\Lambda$ process near threshold. The theoretical predictions for the helicity cross sections $\sigma_{3/2}$, $\sigma_{1/2}$, as well as their ratios, and the angular distributions of π in the $\pi\Lambda$ center-of-mass system are given. It is found that assuming $\Sigma^*(\frac{1}{2}^-)$ exists or not, these physical quantities are distinctly different. So our results could be useful for the investigation of the existence of $\Sigma^*(\frac{1}{2}^-)$ when the experimental data are available in the future.

DOI: 10.1103/PhysRevC.88.024304 PACS number(s): 14.20.Jn, 25.20.Lj, 13.60.Le, 13.60.Rj

I. INTRODUCTION

From studies of baryon spectroscopy and internal structures, the picture of some baryons having large five-quark $qqqq\bar{q}$ fraction was proposed [1–5]. The penta-quark picture can naturally solve some puzzles in classic three-constituent-quark models, for example for the $J^P = \frac{1}{2}^-$ baryons why $N^*(1535)$ is heavier than $\Lambda^*(1405)$ [2]. For the lowest mass strange baryon, the penta-quark models [1,6] predict a $\Sigma^*(\frac{1}{2}^-)$ state with mass about 1360∼1405 MeV which is around the mass, 1385 MeV, of the known $\Sigma^*(\frac{3}{2}^+)$. The studies of Σ^* are of intrinsic interest to check the correctness of penta-quark models, and recently some evidence for the existence of the $\Sigma^*(\frac{1}{2}^-)$ near 1380 MeV has been found through research on the $K^-p \to \Lambda\pi^+\pi^-$ process [7,8] and the $K\Lambda\pi$ [9] and $K\Sigma\pi$ [10] photoproduction processes.

Photoproduction of $K\Sigma^*$ provides a useful tool for understanding baryon spectroscopy and structures. In the early time the limited experimental data on the cross section for $\gamma + p \to K^+ + \Sigma^{*0}(1385)$ have large error bars [11–13]. Only in recent years, the high-statistical experimental data on the $K\Sigma^*$ photoproduction have been made available. The CLAS Collaboration has measured the cross section of $\gamma + p \to K^+ + \Sigma^{*0}(1385)$ with photon energies covering from the threshold up to 4.0 GeV [14]. The LEPS Collaboration has reported the first measurement of the cross section and beam asymmetries of the $\gamma + n \to K^+ + \Sigma^{*-}(1385)$ process, using a linearly polarized photon beam with energy of $E_\gamma = 1.5$–2.4 GeV [15]. Theoretical investigations of $K\Sigma^*$ photoproduction have been presented in Refs. [9,16–18]. In Ref. [18], the t-, s-, and u-channel diagrams as well as the contact term, which are required by gauge invariance, are calculated and are compared with the CLAS data [14]. Though Ref. [18]'s theoretical results of the $K\Sigma^*$ photoproduction cross section agree well with the CLAS data and LEPS data, its prediction for the beam asymmetries greatly deviates from the measurement by the LEPS Collaboration. This obstacle can be solved by including a new $\Sigma^*(\frac{1}{2}^-)$ state with a mass around 1380 MeV, and in this way the experimental data from both the CLAS Collaboration and LEPS Collaboration can be well described as found in Ref. [9].

The existence of $\Sigma^*(\frac{1}{2}^-)$ can also be tested through the experimental measurement of the initial-state polarized $\gamma N \to K^+\Sigma^* \to K^+\pi\Lambda$ process. With the photon circularly polarized and the target of the nucleon polarized along the photon momentum direction, the total helicity may be $\frac{3}{2}$ or $\frac{1}{2}$, corresponding to the spin-parallel and spin-antiparallel state of the photon and nucleon, respectively. In the energy range near threshold, the state of total helicity $\frac{3}{2}$ can only produce $\Sigma^*(\frac{3}{2}^+)$, while the the state of total helicity $\frac{1}{2}$ can produce both $\Sigma^*(\frac{3}{2}^+)$ and $\Sigma^*(\frac{1}{2}^-)$. Theoretically, we can predict the helicity cross section $\sigma_{3/2}$, $\sigma_{1/2}$ and the angular distribution of the final π in the $\pi\Lambda$ center-of-mass (c.m.) system assuming there only exist $\Sigma^*(\frac{3}{2}^+)$ or there exist both $\Sigma^*(\frac{3}{2}^+)$ and $\Sigma^*(\frac{1}{2}^-)$. The ratio of $\frac{\sigma_{3/2}}{\sigma_{1/2}}$ and the angular distribution of π will be different in the two cases, so the existence of $\Sigma^*(\frac{1}{2}^-)$ can be tested by future experimental analyses. In this article, within the framework of the gauge-invariant effective Lagrangian from [9,18], we have made such calculation of the initial-state polarized $\gamma N \to K^+\Sigma^* \to K^+\pi\Lambda$ process taking into account or neglecting the $\Sigma^*(\frac{1}{2}^-)$.

This paper is organized as follows. In Sec. II, the theoretical framework is presented for the initial-state polarized $\gamma N \to K^+\Sigma^* \to K^+\pi\Lambda$ process, where Σ^* include $\Sigma^*(\frac{3}{2}^+)$ and $\Sigma^*(\frac{1}{2}^-)$. In Sec. III, the theoretical predictions for the helicity cross sections $\sigma_{3/2}$, $\sigma_{1/2}$, as well as their ratio, and the angular distribution of the π in the $\pi\Lambda$ c.m. system with or without the $\Sigma^*(\frac{1}{2}^-)$ are presented. We compare and discuss the results of these two cases. In Sec. IV, we give a summary of this work.

II. THEORETICAL FRAMEWORK

The Feynman diagrams for $\gamma N \to K^+\Sigma^* \to K^+\pi\Lambda$ are shown in Fig. 1, where k, p, q, p_π, and p_Λ are the momenta of the incoming photon and nucleon and outgoing K, π, and Λ, respectively, and p' is the momentum of the intermediate Σ^*. Following the strategy of Refs. [9,18], for the reaction $\gamma N \to K^+\Sigma^*(\frac{3}{2}^+) \to K^+\pi\Lambda$ we consider the contribution of the t-channel K meson exchange, the s-channel N and Δ as well as their resonances exchange, the u-channel Λ (for the neutral

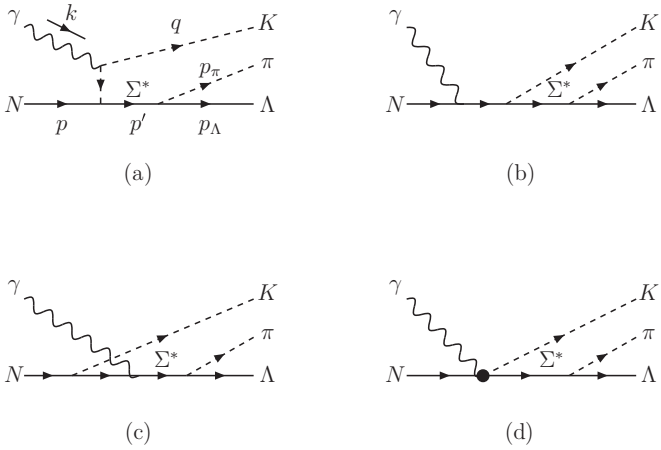

FIG. 1. Feynman diagrams for $\gamma N \to K^+\Sigma^* \to K^+\pi\Lambda$. (a) t channel; (b) s channel; (c) u channel; (d) contact term.

propagator only) and $\Sigma^*(\frac{3}{2}^+)$ exchange, and the contact term. For the reaction $\gamma N \to K^+\Sigma^*(\frac{1}{2}^-) \to K^+\pi\Lambda$, we consider the contribution of the t-channel K meson exchange, the s-channel N exchange, the u-channel $\Sigma^*(\frac{1}{2}^-)$ exchange [and Λ exchange for $\gamma p \to K^+\Sigma^{*0}(\frac{1}{2}^-)$], and the contact term.

The effective Lagrangians and coupling constants relevant to the $\gamma N \to K^+\Sigma^*$ reaction used in this article are taken from Refs. [9,18] and are listed below for completeness, and the interested reader can consult Refs. [9,18] for more details.

For the t-channel K meson exchange:

$$\mathcal{L}_{\gamma KK} = ieA_\mu(K^-\partial^\mu K^+ - \partial^\mu K^- K^+), \tag{1}$$

$$\mathcal{L}_{KN\Sigma^*_{3/2}} = \frac{f_{KN\Sigma^*_{3/2}}}{m_K}\partial_\mu \bar{K}\bar{\Sigma}^{*\mu}_{3/2}\tau N + \text{H.c.}, \tag{2}$$

$$\mathcal{L}_{KN\Sigma^*_{1/2}} = -ig_{KN\Sigma^*_{1/2}}\bar{K}\bar{\Sigma}^*_{1/2}\tau N + \text{H.c.}, \tag{3}$$

with the isospin structure of $K\Sigma^*N$ coupling,

$$\bar{K} = (K^-, \bar{K}^0), \quad \bar{\Sigma}^*\tau = \begin{pmatrix} \bar{\Sigma}^{*0} & \sqrt{2}\bar{\Sigma}^{*+} \\ \sqrt{2}\bar{\Sigma}^{*-} & -\bar{\Sigma}^{*0} \end{pmatrix}, \quad N = \begin{pmatrix} p \\ n \end{pmatrix}, \tag{4}$$

where the coupling constant $f_{KN\Sigma^*_{3/2}} = -3.22 \pm 0.04$ [18] and $g_{KN\Sigma^*_{1/2}} = 1.34 \pm 0.07$ [9].

For the s-channel of nucleon exchange, the effective Lagrangian for the γNN vertex is

$$\mathcal{L}_{\gamma NN} = -e\overline{N}\left(\gamma^\mu A_\mu Q_N - \frac{\kappa_N}{2M_N}\sigma^{\mu\nu}\partial_\nu A_\mu\right)N, \tag{5}$$

where Q_N is the electric charge (in units of e), and κ_N denotes the magnetic moment of the nucleon: $\kappa_n = -1.913$ and $\kappa_p = 2.793$.

The $\gamma N \to K^+\Sigma^*(\frac{3}{2}^+)$ process has s-channel spin-$\frac{3}{2}$ and spin-$\frac{5}{2}$ resonances exchange diagrams, and the effective Lagrangians are

$$\mathcal{L}_{\gamma NR}\left(\frac{3}{2}^\pm\right) = -\frac{ief_1}{2M_N}\bar{N}\Gamma^{(\pm)}_\nu F^{\mu\nu}R_\mu - \frac{ef_2}{(2M_N)^2}\partial_\nu\bar{N}\Gamma^{(\pm)}F^{\mu\nu}R_\mu + \text{H.c.}, \tag{6}$$

$$\mathcal{L}_{\gamma NR}\left(\frac{5}{2}^\pm\right) = \frac{ef_1}{(2M_N)^2}\bar{N}\Gamma^{(\mp)}_\nu\partial^\alpha F^{\mu\nu}R_{\mu\alpha} - \frac{ief_2}{(2M_N)^3}\partial_\nu\bar{N}\Gamma^{(\mp)}\partial^\alpha F^{\mu\nu}R_{\mu\alpha} + \text{H.c.}, \tag{7}$$

and

$$\mathcal{L}_{RK\Sigma^*}\left(\frac{3}{2}^\pm\right) = \frac{h_1}{m_K}\partial^\alpha K\bar{\Sigma}^{*\mu}\Gamma^{(\pm)}_\alpha R_\mu + \frac{ih_2}{(m_K)^2}\partial^\mu\partial^\alpha K\bar{\Sigma}^*_\alpha\Gamma^{(\pm)}R_\mu + \text{H.c.}, \tag{8}$$

$$\mathcal{L}_{RK\Sigma^*}\left(\frac{5}{2}^\pm\right) = \frac{ih_1}{m_K^2}\partial^\mu\partial^\beta K\bar{\Sigma}^{*\alpha}\Gamma^{(\mp)}_\mu R_{\alpha\beta} - \frac{h_2}{(m_K)^3}\partial^\mu\partial^\alpha\partial^\beta K\bar{\Sigma}^*_\mu\Gamma^{(\mp)}R_{\alpha\beta} + \text{H.c.}, \tag{9}$$

where $F^{\mu\nu} = \partial^\mu A^\nu - \partial^\nu A^\mu$, R_μ and $R_{\mu\alpha}$ denote the spin-$\frac{3}{2}$ and spin-$\frac{5}{2}$ fields, respectively, and

$$\Gamma^{(\pm)}_\mu = \begin{pmatrix} \gamma_\mu\gamma_5 \\ \gamma_\mu \end{pmatrix}, \quad \Gamma^{(\pm)} = \begin{pmatrix} \gamma_5 \\ 1 \end{pmatrix}. \tag{10}$$

For the Δ resonances of isospin-$\frac{3}{2}$, the effective Lagrangians have the isospin structure

$$\bar{K}\bar{\Sigma}^*\cdot\mathbf{T}\left(\frac{1}{2},\frac{3}{2}\right)\Delta = \sqrt{3}K^-\bar{\Sigma}^{*+}\Delta^{++} - \sqrt{2}K^-\bar{\Sigma}^{*0}\Delta^+ - K^-\bar{\Sigma}^{*-}\Delta^0 + \bar{K}^0\bar{\Sigma}^{*+}\Delta^+ - \sqrt{2}\bar{K}^0\bar{\Sigma}^{*0}\Delta^0 - \sqrt{3}\bar{K}^0\bar{\Sigma}^{*-}\Delta^-. \tag{11}$$

We consider three two-star-rated resonances in the s channel, $N_{3/2^-}(2120)$, $\Delta_{3/2^-}(1940)$, and $\Delta_{5/2^+}(2000)$, which are the most prominent resonances as stated in Ref. [18]. The coupling constants f_1 and f_2 can be either computed by using Eq. (B3) in Ref. [18] from the helicity amplitudes in the PDG [19] or from the model predictions. For the $\gamma N\Delta$ coupling, we have $f_1 = 4.04 \pm 0.20$ and $f_2 = 3.87 \pm 0.19$ [18]. From the predicted helicity amplitudes in Ref. [20], one has $f_1 = -1.25$ and $f_2 = 1.21$ for the $\gamma pN^*(2120)$ coupling; $f_1 = 0.381$ and $f_2 = -0.256$ for the $\gamma nN^*(2120)$ coupling; $f_1 = 0.39$ and $f_2 = -0.57$ for the $\gamma N\Delta(1940)$ coupling; and $f_1 = -0.68$, $f_2 = -0.062$ for the $\gamma N\Delta(2000)$ coupling [9]. For the $\Delta K\Sigma^*$ coupling, $h_1 = 2.000 \pm 0.006$ and $h_2 = 0$ are obtained from $h_1 = -f_{K\Delta\Sigma^*}/\sqrt{3}$ with $f_{K\Delta\Sigma^*} = -3.46 \pm 0.01$ [21]. For the resonances coupling to the $K\Sigma^*$, the coupling constants h_1 and h_2 can be computed by using Eqs. (B11)–(B18) in Ref. [20] from the model-predicted amplitudes $G(l)$ [22]. One obtains $h_1 = 0.24$ and $h_2 = -0.54$ for the $N^*(2120)K\Sigma^*$ coupling, $h_1 = -0.68$ and $h_2 = 1.0$ for the $\Delta(1940)K\Sigma^*$ coupling, and $h_1 = -1.1$ and $h_2 = 0.21$ for the $\Delta(2000)K\Sigma^*$

coupling [9]. Note that the masses, widths, and coupling constants of the s-channel resonances $N_{3/2^-}(2120)$, $\Delta_{3/2^-}(1940)$, and $\Delta_{5/2^+}(2000)$ are not well constrained by the experiment—hence these parameters have large uncertainties—while near threshold these three resonances' contributions are very small so their uncertainties to our theoretical predictions are negligible.

For the u-channel $\Lambda(1116)$ exchange in the $\gamma p \to K^+\Sigma^{*0}$ reaction, the effective Lagrangians are

$$\mathcal{L}_{\gamma\Lambda\Sigma^*_{3/2}} = -\frac{ief_1}{2M_\Lambda}\bar{\Lambda}\gamma_\nu\gamma_5 F^{\mu\nu}\Sigma^*_{3/2\mu} - \frac{ef_2}{(2M_\Lambda)^2}\partial_\nu\bar{\Lambda}\gamma_5 F^{\mu\nu}\Sigma^*_{3/2\mu} + \text{H.c.}, \quad (12)$$

$$\mathcal{L}_{\gamma\Lambda\Sigma^*_{1/2}} = \frac{eg_{\gamma\Lambda\Sigma^*_{1/2}}}{4\left(M_\Lambda + M_{\Sigma^*_{1/2}}\right)}\bar{\Sigma}^*_{1/2}\gamma_5\sigma_{\mu\nu}\Lambda F^{\nu\mu} + \text{H.c.}, \quad (13)$$

$$\mathcal{L}_{KN\Lambda} = \frac{g_{KN\Lambda}}{M_N + M_\Lambda}\bar{N}\gamma^\mu\gamma_5\Lambda\partial_\mu K + \text{H.c.}, \quad (14)$$

where $f_1 = 4.52 \pm 0.32$, $f_2 = 5.63 \pm 0.45$ are obtained from the decay width $\Gamma(\Sigma^*_{3/2} \to \Lambda\gamma)$ and $g_{\gamma\Lambda\Sigma^*_{1/2}} = 1.16$. From the flavor SU(3) symmetry relation, one has $g_{KN\Lambda} = -13.24 \pm 1.06$ [18].

For the u-channel Σ^* exchange, the effective Lagrangians are

$$\mathcal{L}_{\gamma\Sigma^*_{1/2}\Sigma^*_{1/2}} = -e\overline{\Sigma}^*_{1/2}\left(\gamma^\mu A_\mu Q_{\Sigma^*_{1/2}} - \frac{\kappa_{\Sigma^*_{1/2}}}{2M_N}\sigma^{\mu\nu}\partial_\nu A_\mu\right)\Sigma^*_{1/2}, \quad (15)$$

$$\mathcal{L}_{\gamma\Sigma^*_{3/2}\Sigma^*_{3/2}} = e\bar{\Sigma}^*_{3/2\mu}A_\alpha\Gamma^{\alpha,\mu\nu}_{\gamma\Sigma^*_{3/2}}\Sigma^*_{3/2\nu}, \quad (16)$$

with

$$A_\alpha\Gamma^{\alpha,\mu\nu}_{\gamma\Sigma^*_{3/2}} = Q_{\Sigma^*_{3/2}}A_\alpha\left(g^{\mu\nu}\gamma^\alpha - \frac{1}{2}(\gamma^\mu\gamma^\nu\gamma^\alpha + \gamma^\alpha\gamma^\mu\gamma^\nu)\right) - \frac{\kappa_{\Sigma^*_{3/2}}}{2M_N}\sigma^{\alpha\beta}\partial_\beta A_\alpha g^{\mu\nu}, \quad (17)$$

where Q_{Σ^*} is the electric charge (in units of e), and κ_{Σ^*} denotes the anomalous magnetic moment of Σ^*: $\kappa_{\Sigma^{*0}_{3/2}} = 0.36$ and $\kappa_{\Sigma^{*-}_{3/2}} = -2.43$ are taken from the quark model [23], and $\kappa_{\Sigma^{*0}_{1/2}} = -0.43$ and $\kappa_{\Sigma^{*-}_{1/2}} = -1.74$ are predicted by the penta-quark model [6].

To take account of the off-shell effects, every vertex of these channels has been given a form factor. For the t-channel K meson exchange, we use the form factor [18]

$$F_M = \frac{\Lambda_M^2 - m_K^2}{\Lambda_M^2 - q_t^2}, \quad (18)$$

where $q_t = k - q$. We adopt $\Lambda_M = 0.83$ GeV for $\Sigma^*_{3/2}$ and $\Lambda_M = 1.6$ GeV for $\Sigma^*_{1/2}$ [9]. For the s-channel N and Δ exchange, the u-channel processes, and the $\Sigma^*\Lambda\pi$ vertex, we adopt the form factor [18]

$$F_B\left(q_{ex}^2, M_{ex}\right) = \frac{\Lambda_B^4}{\Lambda_B^4 + \left(q_{ex}^2 - M_{ex}^2\right)^2}, \quad (19)$$

where the q_{ex} and M_{ex} are the 4-momentum and the mass of the exchanged hadron, respectively. For the s-channel resonances exchange, the form factor is

$$F_B\left(q_s^2, M_R\right) = \exp\left(-\frac{\left(q_s^2 - M_R^2\right)^2}{\Lambda_B^4}\right), \quad (20)$$

with the cutoff parameter $\Lambda_B = 1.0$ GeV [18]. Note in this paper that we only study the near-threshold physics so the difference between the Gaussian form factors and the more justifiable dipole form factors is small. We have checked that using the dipole form factors for all baryons, the numerical differences are within 1%.

The contact term in Fig. 1(d) is required to keep the full amplitude gauge invariant. For the process $\gamma p \to K^+\Sigma^{*0}_{3/2}$, we adopt the contact current [18,24]

$$M_c^{\mu\nu} = ie\frac{f_{KN\Sigma^*_{3/2}}}{m_K}(g^{\mu\nu}f_t - q^\mu C^\nu), \quad (21)$$

where C^ν is expressed as

$$C^\nu = -(2q-k)^\nu\frac{f_t - 1}{t - m_K^2}[1 - h(1 - f_s)] - (2p + k)^\nu\frac{f_s - 1}{s - M_N^2}[1 - h(1 - f_t)]. \quad (22)$$

Here the Lorenz indexes μ and ν couple to that of $\Sigma^*_{3/2}$ and the photon, respectively; $f_t = F_M^2$ and $f_s = F_B^2(s, M_N)$ are form factors squared; and $t = q_t^2$ and $s = q_s^2$; h is a parameter to be fitted to experiments; and $h = 1$ is used in Ref. [18]. For the process $\gamma p \to K^+\Sigma^{*0}_{1/2}$, the contact current is

$$M_c^\nu = ieg_{KN\Sigma^*_{1/2}}C^\nu, \quad (23)$$

where $h = 1$ is adopted. For the reaction $\gamma n \to K^+\Sigma^{*-}_{3/2}$, the contact current is [24]

$$M_c^{\mu\nu} = ie\sqrt{2}\frac{f_{KN\Sigma^*_{3/2}}}{m_K}(g^{\mu\nu}f_t - q^\mu C^\nu), \quad (24)$$

with

$$C^\nu = -(2q-k)^\nu\frac{f_t - 1}{t - m_K^2}[1 - h(1 - f_u)] + (2p' - k)^\nu\frac{f_u - 1}{u - M_{\Sigma^*}^2}[1 - h(1 - f_t)], \quad (25)$$

where $f_u = F_B^2(u, M_\Sigma^*)$ is the form factor squared, and $u = q_u^2$ is the squared momentum transfer for the u channel. According to Ref. [9], $h = 1.11$ is taken assuming there only exist $\Sigma^*(\frac{3}{2}^+)$, and $h = 1$ is used if there exist both $\Sigma^*(\frac{3}{2}^+)$ and $\Sigma^*(\frac{1}{2}^-)$. For the $\gamma n \to K^+\Sigma^{*-}(\frac{1}{2}^-)$ process, we adopt the contact current:

$$M_c^\nu = ie\sqrt{2}g_{KN\Sigma^*_{1/2}}C^\nu, \quad (26)$$

where C^ν is expressed as Eq. (25), and here $h = 1$ is taken.

All the ingredients of the $\gamma N \to K^+\Sigma^*$ reaction are given above, and now we list the effective Lagrangians of the $\Sigma^*\Lambda\pi$ vertex [8,25]:

$$\mathcal{L}_{\Lambda\pi\Sigma^*_{3/2}} = g_{\Lambda\pi\Sigma^*_{3/2}}\bar{\Lambda}\Sigma^{*\mu}_{3/2}\partial_\mu\pi + \text{H.c.}, \quad (27)$$

$$\mathcal{L}_{\Lambda\pi\Sigma^*_{1/2}} = -ig_{\Lambda\pi\Sigma^*_{1/2}}\overline{\Sigma}^*_{1/2}\Lambda\pi + \text{H.c.}, \quad (28)$$

where $g_{\Lambda\pi\Sigma^*_{3/2}} = 9.16 \pm 0.66$ is obtained from the decay widths of $\Gamma(\Sigma^*_{3/2} \to \Lambda\pi)$ [19], and $g_{\Lambda\pi\Sigma^*_{1/2}} = 2.12 \pm 0.33$ is obtained assuming the fitted result of the $\Sigma^*_{1/2}$ decay width in Ref. [7] is contributed totally by the $\Lambda\pi$ channel.

Furthermore, we need the propagators of intermediate particles to calculate the Feymann diagrams. For t-channel exchange K meson, the propagator is

$$G_{K(q_t)} = 1/\left(q_t^2 - m_K^2\right). \tag{29}$$

For the spin-1/2, spin-3/2, and spin-5/2 baryons the propagators are respectively

$$G^{1/2}_{R(p)} = \frac{\not{p} + m}{p^2 - m^2}, \tag{30}$$

$$G^{3/2}_{R(p)} = \frac{\not{p} + m}{p^2 - m^2}\left(-g^{\mu\nu} + \frac{\gamma^\mu\gamma^\nu}{3} + \frac{\gamma^\mu p^\nu - \gamma^\nu p^\mu}{3m} + \frac{2p^\mu p^\nu}{3m^2}\right), \tag{31}$$

$$G^{5/2}_{R(p)} = \frac{\not{p} + m}{p^2 - m^2} S_{\alpha\beta\mu\nu}(p, m), \tag{32}$$

where

$$S_{\alpha\beta\mu\nu}(p, m) = \tfrac{1}{2}(\bar{g}_{\alpha\mu}\bar{g}_{\beta\nu} + \bar{g}_{\alpha\nu}\bar{g}_{\beta\mu}) - \tfrac{1}{5}\bar{g}_{\alpha\beta}\bar{g}_{\mu\nu} - \tfrac{1}{10}(\bar{\gamma}_\alpha\bar{\gamma}_\mu\bar{g}_{\beta\nu} + \bar{\gamma}_\alpha\bar{\gamma}_\nu\bar{g}_{\beta\mu} + \bar{\gamma}_\beta\bar{\gamma}_\mu\bar{g}_{\alpha\nu} + \bar{\gamma}_\beta\bar{\gamma}_\nu\bar{g}_{\alpha\mu}), \tag{33}$$

with

$$\bar{g}_{\mu\nu} = g_{\mu\nu} - \frac{p_\mu p_\nu}{m^2}, \quad \bar{\gamma}_\mu = \gamma_\mu - \frac{p_\mu}{m^2}\not{p}. \tag{34}$$

For the intermediate resonances with sizable width Γ, namely $N_{3/2^-}(2120)$, $\Delta_{3/2^-}(1940)$, $\Delta_{5/2^+}(2000)$, $\Sigma^*(\frac{3}{2}^+)$, and $\Sigma^*(\frac{1}{2}^-)$, we replace the denominator $\frac{1}{p^2-m^2}$ in the propagators with $\frac{1}{p^2-m^2+im\Gamma}$, and replace m in the rest of the propagators with $\sqrt{p^2}$. These decay widths are taken from Refs. [7,9], which are within the PDG range, $\Gamma_{N^*(2120)} = 0.25$ GeV, $\Gamma_{\Delta(1940)} = 0.15$ GeV, $\Gamma_{\Delta(2000)} = 0.15$ GeV, $\Gamma_{\Sigma^*(\frac{3}{2}^+)} = 0.035 \pm 0.005$ GeV, and $\Gamma_{\Sigma^*(\frac{1}{2}^-)} = 0.119^{+0.055}_{-0.035}$ GeV. Since previous investigation indicates that the mass of the new $\Sigma^*(\frac{1}{2}^-)$ is around $\Sigma^*(\frac{3}{2}^+)$ [7–9], here we assume its mass be the same as $\Sigma^*(\frac{3}{2}^+)$. Note there are ambiguities when dealing with the high-spin off-shell particles [26–28], since here we are using a tree-level approach and possible effects might be partially encoded into the phenomenological coupling constants which are constrained by the experiments. Also, these uncertainties of off-shell effects might be partially effectively included into the form factors, and in this paper the values of the cutoff parameters Λ_M and Λ_B are taken from Refs. [15,18], gotten by fitting the $\gamma p \to K^+\Sigma^{*0}$ data. So the description of high-spin particles used here can properly explore the phenomenological physics.

The differential cross section for $\gamma N \to K^+\Sigma^* \to K^+\pi\Lambda$ can be expressed as

$$d\sigma_{\gamma N\to K^+\Sigma^*\to K^+\pi\Lambda} = \frac{|\mathbf{q}||\mathbf{p}_\pi||\bar{\mathcal{M}}|^2}{(2\pi)^5 32 s|\mathbf{k}|} d\Omega d\Omega' dm_{\pi\Lambda}, \tag{35}$$

where $\mathbf{k}$ and $\mathbf{q}$ denote the 3-momenta of photon and K^+ in the c.m. frame, respectively, and $\mathbf{p}_\pi$ is the 3-momenta of the produced π in the Σ^* rest frame; $d\Omega = 2\pi d\cos\theta$, and θ denotes the angle of the outgoing K^+ relative to beam direction in the c.m. frame; $d\Omega' = d\cos\theta' d\phi'$ is the sphere space of the outgoing π in the Σ^* rest frame, and θ' is the angle between the π direction and the K^+ direction in the c.m system of the $\pi\Lambda$; $m_{\pi\Lambda}$ is the invariant mass of π and Λ, which satisfies $m^2_{\pi\Lambda} = (p_\pi + p_\Lambda)^2$. With the z axis being the direction of motion of the photon and the x-z plane being the reaction plane, the polarization vectors for right- and left-handed photons are

$$\vec{\epsilon}_R = -\frac{1}{\sqrt{2}}(\vec{\epsilon}_x + i\vec{\epsilon}_y), \quad \vec{\epsilon}_L = +\frac{1}{\sqrt{2}}(\vec{\epsilon}_x - i\vec{\epsilon}_y). \tag{36}$$

For the polarized nucleon we use the projection operators [29]

$$u(p)\bar{u}(p) = (\not{p} + m_N)\tfrac{1}{2}(1 + 2\lambda\gamma_5\not{s}), \tag{37}$$

where $\lambda = \pm\frac{1}{2}$ is the helicity of the nucleon and $s = (\frac{|\vec{p}|}{m_N}, \frac{E_N}{m_N}\frac{\vec{p}}{|\vec{p}|})$.

III. RESULTS AND DISCUSSION

With the formalism and ingredients given above, we compute the helicity cross section $\sigma_{3/2}$ and $\sigma_{1/2}$, corresponding to spin-parallel and spin-antiparallel states of the photon and nucleon, respectively, for the $\gamma N \to K^+\Sigma^* \to K^+\pi\Lambda$ process assuming there only exists $\Sigma^*(\frac{3}{2}^+)$ or there exist both $\Sigma^*(\frac{3}{2}^+)$ and $\Sigma^*(\frac{1}{2}^-)$. The cross sections versus excess energy in the c.m. frame, Q$= \sqrt{s} - \sqrt{s}_{\text{threshold}}$, are shown in Fig. 2. In Fig. 3, the behavior of the ratios of $\sigma_{3/2}/\sigma_{1/2}$ is given. The error bands are computed in this way: First we compute the maximum and the minimum of each theoretical prediction with the coupling constants within the range of error, then we take (maximum − minimum)/2 as the error bar of corresponding prediction.

Through analysis we find that the contact terms and the u-channel Λ exchange give the most important contributions to the $\gamma p \to K^+\Sigma^{*0}(\frac{3}{2}^+) \to K^+\pi^0\Lambda$ process, while their interference term enhances and reduces the total cross section for $\sigma_{3/2}$ and $\sigma_{1/2}$, respectively, so the ratio of $\sigma_{3/2}/\sigma_{1/2}$ for the pure $\Sigma^*(\frac{3}{2}^+)$ produced process is about 40 as in Fig. 3(a). For the $\gamma p \to K^+\Sigma^{*0}(\frac{1}{2}^-) \to K^+\pi^0\Lambda$ process, $\sigma_{1/2}$ comes mainly from the t-channel K exchange and the s-channel N exchange, while in $\sigma_{3/2}$ the s-channel N exchange's contribution is suppressed due to angular momentum conservation so $\sigma_{1/2}$ is larger than $\sigma_{3/2}$. Assuming there exist both $\Sigma^*(\frac{3}{2}^+)$ and $\Sigma^*(\frac{1}{2}^-)$, the ratio of $\sigma_{3/2}/\sigma_{1/2}$ is about 3 which is distinct from that assuming only $\Sigma^*(\frac{3}{2}^+)$ exist, which can be seen in Fig. 3(a).

For the $\gamma n \to K^+\Sigma^{*-}(\frac{3}{2}^+) \to K^+\pi^-\Lambda$ process, the contact term plays the major role and its contribution to the total cross section is two orders larger than those from other channels, so the ratio of $\sigma_{3/2}/\sigma_{1/2}$ mainly depends on the behavior of the contact term. For the $\gamma n \to K^+\Sigma^{*-}(\frac{1}{2}^-) \to K^+\pi^-\Lambda$ process, the major contribution is from the t-channel

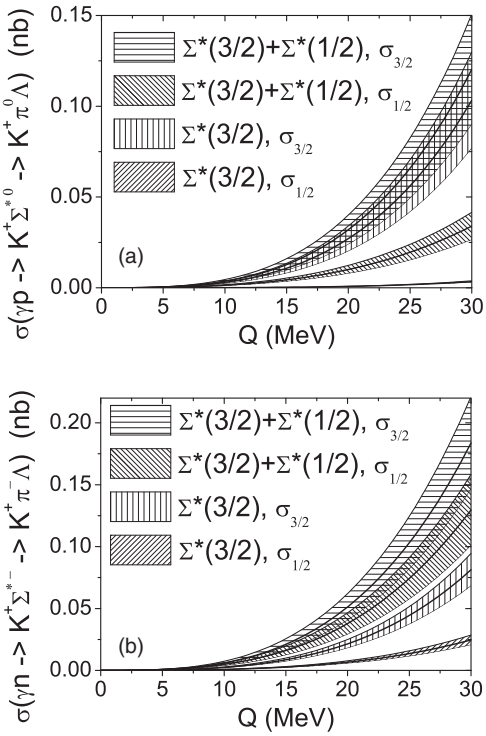

FIG. 2. Predictions for the helicity cross sections contributed from $\Sigma^*(\frac{3}{2}^+)$ and the sum of $\Sigma^*(\frac{3}{2}^+)$ and $\Sigma^*(\frac{1}{2}^-)$ for (a) $\gamma p \to K^+\Sigma^{*0} \to K^+\pi^0\Lambda$ and (b) $\gamma n \to K^+\Sigma^{*-} \to K^+\pi^-\Lambda$ processes. The shaded areas correspond to the error bands.

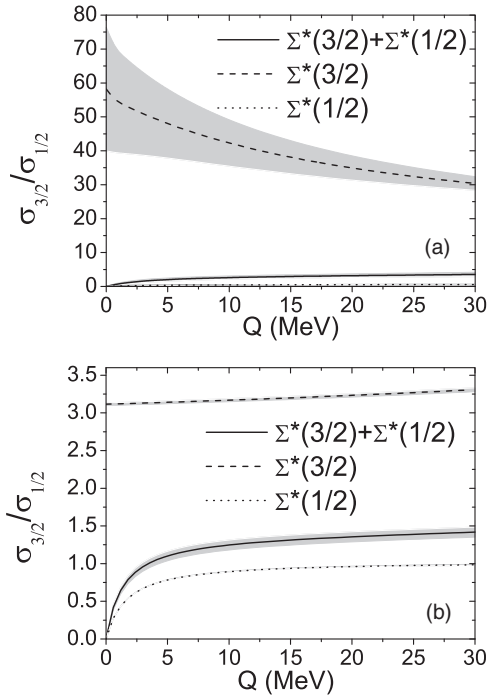

FIG. 3. Predictions for the ratios of $\sigma_{3/2}/\sigma_{1/2}$ assuming there exist only $\Sigma^*(\frac{3}{2}^+)$ (dashed), or only $\Sigma^*(\frac{1}{2}^-)$ (dotted), or both of them (solid) for (a) $\gamma p \to K^+\Sigma^{*0} \to K^+\pi^0\Lambda$ and (b) $\gamma n \to K^+\Sigma^{*-} \to K^+\pi^-\Lambda$ processes. The shaded areas correspond to the error bands.

K exchange. As can be seen in Figs. 3(a) and 3(b), the ratios of $\sigma_{3/2}/\sigma_{1/2}$ from pure $\Sigma^*(\frac{1}{2}^-)$ are zero at threshold as expected, while they sharply rise and reach about one when $Q = 10$ MeV. This is because the amplitude of the major t-channel K exchange in $\Sigma^*(\frac{1}{2}^-)$ produced reactions is proportional to the component of the photon polarization vector parallel to the reaction plane, and its contributions to the total cross section are the same for right- and left-handed photons. According to our calculated results, the $\Sigma^*(\frac{1}{2}^-)$ produced cross sections are larger than those produced by $\Sigma^*(\frac{3}{2}^+)$, so taking account of the $\Sigma^*(\frac{1}{2}^-)$ or not, both the total cross section $\sigma_{3/2}$ and $\sigma_{1/2}$ are different, as shown in Fig. 2(b). Also, in Fig. 3(b), the ratios of $\sigma_{3/2}/\sigma_{1/2}$ are different assuming there exist both $\Sigma^*(\frac{3}{2}^+)$ and $\Sigma^*(\frac{1}{2}^-)$ or only exist $\Sigma^*(\frac{3}{2}^+)$.

Another way to investigate the spin of the Σ^* is to utilize the angular distribution of the π in the $\pi\Lambda$ center-of-mass system. Near threshold, the final $\pi\Lambda$ state is in the relative p wave from the decay of $\Sigma^*(\frac{3}{2}^+)$ and is in the relative s wave from the decay of $\Sigma^*(\frac{1}{2}^-)$. So the angular distribution is expected to be of the form $(a + b\cos\theta'^2)$ for the pure $\Sigma^*(\frac{3}{2}^+)$ and a flat constant distribution is predicted for pure $\Sigma^*(\frac{1}{2}^-)$. In Figs. 4 and 5, we show the angular distribution of the π in the $\pi\Lambda$ center-of-mass system for the $\gamma N \to K^+\Sigma^* \to K^+\pi\Lambda$ process assuming there exist only $\Sigma^*(\frac{3}{2}^+)$ and there exist both $\Sigma^*(\frac{3}{2}^+)$ and $\Sigma^*(\frac{1}{2}^-)$ at $Q = 20$ MeV, respectively. Note that here we choose the energy $Q = 20$ MeV just as an example, and the behaviors of the angular distributions do not change significantly near threshold. As illustrated in Fig. 4, the shapes of angular distributions for pure $\Sigma^*(\frac{3}{2}^+)$ agree well with the expectations. We also have checked that the predictions for

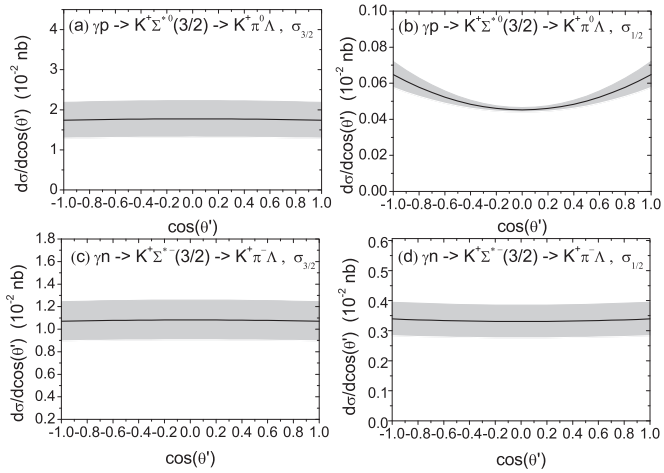

FIG. 4. Predictions for the angular distribution of final π of the $\gamma N \to K^+\Sigma^*(\frac{3}{2}^+) \to K^+\pi\Lambda$ process, where θ' is the angle between the outgoing π direction and K direction in the c.m. system of $\pi\Lambda$. (a) and (b) denote $\sigma_{3/2}$ and $\sigma_{1/2}$, respectively, for $\gamma p \to K^+\Sigma^{*0}(\frac{3}{2}^+) \to K^+\pi^0\Lambda$ process. (c) and (d) denote $\sigma_{3/2}$ and $\sigma_{1/2}$, respectively, for $\gamma n \to K^+\Sigma^{*-}(\frac{3}{2}^+) \to K^+\pi^-\Lambda$ process. The shaded areas correspond to the error bands.

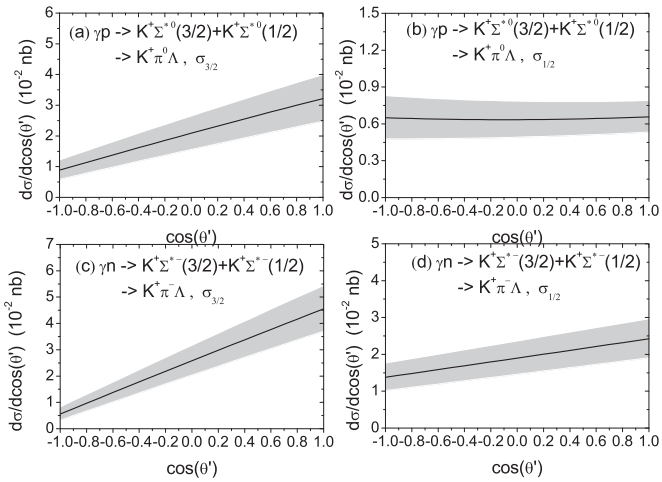

FIG. 5. Predictions for the angular distribution of final π of the $\gamma N \to K^+\Sigma^* \to K^+\pi\Lambda$ process, where Σ^* include $\Sigma^*(\frac{3}{2}^+)$ and $\Sigma^*(\frac{1}{2}^-)$. (a) and (b) denote $\sigma_{3/2}$ and $\sigma_{1/2}$, respectively, for $\gamma p \to K^+\Sigma^{*0} \to K^+\pi^0\Lambda$ process. (c) and (d) denote $\sigma_{3/2}$ and $\sigma_{1/2}$, respectively, for $\gamma n \to K^+\Sigma^{*-} \to K^+\pi^-\Lambda$ process. The shaded areas correspond to the error bands.

the angular distributions from pure $\Sigma^*(\frac{1}{2}^-)$ are flat constants, and we do not illustrate them individually in the figures. The differential cross section contributed by the interference terms of the $\Sigma^*(\frac{3}{2}^+)$ and $\Sigma^*(\frac{1}{2}^-)$ are linear functions of $\cos\theta'$, and we find they change much more rapidly than the corresponding pure $\Sigma^*(\frac{3}{2}^+)$ terms in the $\gamma p \to K^+\Sigma^{*0} \to K^+\pi^0\Lambda$ process for $\sigma_{3/2}$, and in the $\gamma n \to K^+\Sigma^{*-} \to K^+\pi^-\Lambda$ process for $\sigma_{3/2}$ and $\sigma_{1/2}$, so in these reactions the interference terms mainly determine the shapes of the angular distributions as shown in Figs. 5(a), 5(c), and 5(d). In the $\gamma p \to K^+\Sigma^{*0} \to K^+\pi^0\Lambda$ process for $\sigma_{1/2}$, the interference term changes more slowly than the pure $\Sigma^*(\frac{3}{2}^+)$ term so the shape of the angular distribution deviates slightly from that of pure $\Sigma^*(\frac{3}{2}^+)$, as can be seen in Fig. 5(b).

IV. SUMMARY

In this paper, we study the reactions $\gamma N \to K^+\Sigma^*(1385) \to K^+\pi\Lambda$ near threshold within an effective Lagrangian approach. Recent studies indicate that near the mass of $\Sigma^*(\frac{3}{2}^+)$, another Σ^* state with $J^P = \frac{1}{2}^-$ may exits. The spin of Σ^* can be investigated in the $K\Sigma^*$ photoproduction process using circularly polarized photons and a target of polarized nucleons. Taking account of the $\Sigma^*(\frac{1}{2}^-)$ or not, we compute the helicity cross sections $\sigma_{3/2}$ and $\sigma_{1/2}$, which correspond to spin-parallel and spin-antiparallel states of the photon and nucleon respectively, and their ratios. Also we give the predictions for the angular distributions of the π in the $\pi\Lambda$ c.m. system. Through the analysis, we find that the $\Sigma^*(\frac{1}{2}^-)$ and the interference term of $\Sigma^*(\frac{3}{2}^+)$ and $\Sigma^*(\frac{1}{2}^-)$ play significant roles near threshold, such that the ratios of $\sigma_{3/2}/\sigma_{1/2}$ and the angular distribution of the π are distinctly different assuming that the $\Sigma^*(\frac{1}{2}^-)$ exists or not. The results of this work may be useful for identification of $\Sigma^*(\frac{1}{2}^-)$ when the experimental data are available in the future.

ACKNOWLEDGMENTS

We acknowledge Eulogio Oset for the suggestion to start this work and for carefully reading through the manuscript. We also thank Puze Gao, Jia-jun Wu, and Jian-ping Dai for helpful discussions. This work is supported in part by the National Natural Science Foundation of China under Grants No. 11035006, No. 11121092, and No. 11261130311 (CRC110 by DFG and NSFC), the Chinese Academy of Sciences under Project No. KJCX2-EW-N01, and the Ministry of Science and Technology of China (2009CB825200).

[1] C. Helminen and D. O. Riska, Nucl. Phys. A **699**, 624 (2002).
[2] B. S. Zou, Eur. Phys. J. A **35**, 325 (2008); Int. J. Mod. Phys. A **21**, 5552 (2006).
[3] B. C. Liu and B. S. Zou, Phys. Rev. Lett. **96**, 042002 (2006); **98**, 039102 (2007).
[4] C. S. An, Q. B. Li, D. O. Riska, and B. S. Zou, Phys. Rev. C **74**, 055205 (2006); **75**, 069901(E) (2007).
[5] C. S. An, Nucl. Phys. A **797**, 131 (2007); **801**, 82 (2008).
[6] A. Zhang *et al.*, High Energy Phys. Nucl. Phys. **29**, 250 (2005), arXiv:hep-ph/0403210.
[7] J. J. Wu, S. Dulat, and B. S. Zou, Phys. Rev. D **80**, 017503 (2009).
[8] J. J. Wu, S. Dulat, and B. S. Zou, Phys. Rev. C **81**, 045210 (2010).
[9] P. Z. Gao, J. J. Wu, and B. S. Zou, Phys. Rev. C **81**, 055203 (2010).
[10] K. Moriya *et al.* (CLAS Collaboration), Phys. Rev. C **87**, 035206 (2013).
[11] J. H. R. Crouch *et al.* (Cambridge Bubble Chamber Group), Phys. Rev. **156**, 1426 (1967).
[12] R. Erbe *et al.* (DESY Bubble Chamber Group), Nuovo Cimento A **49**, 504 (1967).
[13] R. Erbe *et al.* (ABBHHM Collaboration), Phys. Rev. **188**, 2060 (1969).
[14] L. Guo and D. P. Weygand (CLAS Collaboration), in *Proceedings of the International Workshop on the Physics of Excited Baryons (NSTAR05)*, edited by S. Capstick, V. Crede, and P. Eugenio (World Scientific, Singapore, 2006), pp. 306–309.
[15] K. Hicks *et al.* (LEPS Collaboration), Phys. Rev. Lett. **102**, 012501 (2009).
[16] M. F. M. Lutz and M. Soyeur, Nucl. Phys. A **748**, 499 (2005).
[17] M. Döring, E. Oset, and D. Strottman, Phys. Lett. B **639**, 59 (2006); Phys. Rev. C **73**, 045209 (2006).
[18] Y. Oh, C. M. Ko, and K. Nakayama, Phys. Rev. C **77**, 045204 (2008).

[19] J. Beringer *et al*. (Particle Data Group), Phys. Rev. D **86**, 010001 (2012).
[20] S. Capstick, Phys. Rev. D **46**, 2864 (1992).
[21] Y. Oh, K. Nakayama, and T.-S. H. Lee, Phys. Rep. **423**, 49 (2006).
[22] S. Capstick and W. Roberts, Phys. Rev. D **58**, 074011 (1998).
[23] D. B. Lichtenberg, Phys. Rev. D **15**, 345 (1977).
[24] H. Haberzettl, K. Nakayama, and S. Krewald, Phys. Rev. C **74**, 045202 (2006).
[25] P. Z. Gao, J. Shi, and B. S. Zou, Phys. Rev. C **86**, 025201 (2012).
[26] V. Pascalutsa and R. Timmermans, Phys. Rev. C **60**, 042201 (1999).
[27] T. Vrancx, L. De Cruz, J. Ryckebusch, and P. Vancraeyveld, Phys. Rev. C **84**, 045201 (2011).
[28] G. Vereshkov and N. Volchanskiy, Phys. Rev. C **87**, 035203 (2013).
[29] J. D. Bjorken and S. D. Drell, *Relativistic Quantum Mechanics* (McGraw-Hill, New York, 1965).